The microtubule plus-end tracking protein Bik1 is required for chromosome congression

Alexander Julner, Marjan Abbasi, and Victoria Menéndez-Benito*
Department of Biosciences and Nutrition, Karolinska Institutet, SE-141 83, Huddinge, Sweden

ABSTRACT **During mitosis, sister chromatids congress on both sides of the spindle equator to facilitate the correct partitioning of the genomic material. Chromosome congression requires a finely tuned control of microtubule dynamics by the kinesin motor proteins. In *Saccharomyces cerevisiae*, the kinesin proteins Cin8, Kip1, and Kip3 have a pivotal role in chromosome congression. It has been hypothesized that additional proteins that modulate microtubule dynamics are involved. Here, we show that the microtubule plus-end tracking protein Bik1—the budding yeast ortholog of CLIP-170—is essential for chromosome congression. We find that nuclear Bik1 localizes to the kinetochores in a cell cycle–dependent manner. Disrupting the nuclear pool of Bik1 with a nuclear export signal (Bik1-NES) leads to slower cell-cycle progression characterized by a delayed metaphase–anaphase transition. Bik1-NES cells have mispositioned kinetochores along the spindle in metaphase. Furthermore, using proximity-dependent methods, we identify Cin8 as an interaction partner of Bik1. Deleting CIN8 reduces the amount of Bik1 at the spindle. In contrast, Cin8 retains its typical bilobed distribution in the Bik1-NES mutant and does not localize to the unclustered kinetochores. We propose that Bik1 functions with Cin8 to regulate kinetochore–microtubule dynamics for correct kinetochore positioning and chromosome congression.**

Monitoring Editor
Kerry Bloom
University of North Carolina, Chapel Hill

Received: Oct 18, 2021
Revised: Feb 10, 2022
Accepted: Feb 24, 2022

INTRODUCTION

Cell division relies on the accurate segregation of sister chromatids to generate functional daughter cells. Before segregation, sister chromatids are positioned at the spindle equator through a process known as chromosome congression that culminates with metaphase plate formation in metazoans (reviewed in [Maiato *et al.*, 2017]). The establishment of a metaphase plate forces all the chromosomes to segregate from the same starting position, thereby contributing to faithful segregation. Despite the relevance of chromosome congression, its molecular mechanisms remain unclear.

The budding yeast *Saccharomyces cerevisiae* is an appealing *S. cerevisiae* model organism for studying spindle dynamics because it is amenable to genetic engineering and has a relatively simple spindle. *S. cerevisiae* has 16 chromosomes. After duplication, each sister chromatid is linked by a kinetochore to a single kinetochore microtubule emanating from the spindle pole body (SPB), the yeast centrosome (Winey and O'Toole, 2001). Each SPB also gives rise to a few interpolar microtubules (starting with around six and ending with two interpolar microtubules from each SPB), with plus-ends that overlap at the middle of the spindle (Peterson and Ris, 1976; Winey *et al.*, 1995; O'Toole *et al.*, 1999). In prometaphase, kinetochores congress in two opposite clusters near the spindle equator, equidistant from the SPBs. As in metazoan cells, this appears to occur before biorientation of sister chromatids (Marco *et al.*, 2013).

Several studies have shown that kinetochore microtubules are regulated in a length-dependent manner (Sprague *et al.*, 2003; Gardner *et al.*, 2005; Pearson *et al.*, 2006). Short microtubules tend to grow, whereas long microtubules that extend toward the spindle equator are destabilized and depolymerize. As sister chromatids are held together by cohesin, depolymerization of kinetochore microtubules generates tension, mediated by the Ndc80 and Dam1 complexes' ability to track the dynamic tips of the kinetochore microtubules (Powers *et al.*, 2009; Suzuki *et al.*, 2016).

This article was published online ahead of print in MBoC in Press (http://www.molbiolcell.org/cgi/doi/10.1091/mbc.E21-10-0500) on March 2, 2022.

Competing financial interests: The authors declare no competing financial interests.

*Address correspondence to: Victoria Menéndez-Benito (victoria.menendez.benito@ki.se).

Abbreviations used: BiFC, bimolecular fluorescence complementation; NES, nuclear export signal; sfGFP, superfolder GFP; SPB, spindle pole body; +TIPs, microtubule plus-end tracking proteins.

Name	% coverage	Unique peptides
STU2	72.33	104
BIM1	67.00	21
CIN8	50.67	46
KIP2	49.33	28
KAR9	47.33	26
KIP1	38.67	28
KAR3	38.67	23
CIK1	22.67	10
VIK1	21.00	10
KIP3	15.33	6

TABLE 1: A subset of the protein interactors of Bik1-FLAG (See Data S1 for a complete list).

Kinesin motors—proteins that move along microtubules powered by the hydrolysis of adenosine triphosphate (ATP)—are involved in chromosome congression in several organisms (see Maiato *et al.*, 2017, Table 1). In budding yeast, the deletion of the kinesins Cin8, Kip3, and, to a lesser extent, Kip1 results in declustering of kinetochores (Tytell and Sorger, 2006; Gardner *et al.*, 2008; Wargacki *et al.*, 2010; Marco *et al.*, 2013). Cin8 and Kip3 have been shown to act as length-dependent microtubule depolymerases, promoting catastrophe of long microtubules (Varga *et al.*, 2006; Gardner *et al.*, 2008; Su *et al.*, 2011).

It has long been speculated that other microtubule-associated proteins could play a role in chromosome congression (Kops *et al.*, 2010). Specifically, microtubule plus-end tracking proteins (+TIPs) are interesting candidates, because they accumulate at kinetochore microtubule plus-ends and regulate their dynamics (reviewed in Akhmanova and Steinmetz, 2010). Bik1, the yeast ortholog of CLIP-170, is a +TIP protein that exists in cytoplasmic and nuclear pools within the cell (Carvalho *et al.*, 2004). The cytoplasmic pool is important for mitotic spindle positioning through both the Kar9 and the dynein pathways (reviewed in Miller *et al.*, 2006). First, Bik1 promotes phosphorylation of Kar9 for asymmetric localization at the old SPB (Moore *et al.*, 2006). Kar9, together with the +TIP protein Bim1 and the actin-guided myosin motor protein Myo2, mediates the capture of astral microtubules at the bud cortex, contributing to spindle alignment and nuclear migration (Xiang, 2018). During anaphase, Bik1 is transported by the kinesin Kip2 to the plus-ends of astral microtubules, where it facilitates the recruitment of dynein (Carvalho *et al.*, 2004; Roberts *et al.*, 2014). Dynein is a minus end–directed motor and will pull the spindle, resulting in nuclear migration to the bud.

The nuclear pool of Bik1 is associated with the spindle at SPBs and kinetochores (Carvalho *et al.*, 2004; Lin *et al.*, 2001), but its function is not well understood. Early studies found that deleting BIK1 results in cells with short or nondetectable astral microtubules (Berlin *et al.*, 1990). In contrast, cells overexpressing Bik1 display short spindle microtubules and long astral microtubules. In this study, we investigate the nuclear function of Bik1 and its role in chromosome congression and cell cycle progression.

RESULTS AND DISCUSSION

Bik1 localizes to kinetochores in a cell cycle–dependent manner

To better understand the nuclear pool of Bik1, we first explored the localization of the protein at different stages of the cell cycle. We used cells expressing Bik1-superfolder GFP (sfGFP), mTurquoise Tub1 (alpha tubulin, microtubule marker), and either Ndc80-TagRFP-T (kinetochore marker) or Spc42-TagRFP-T (SPB marker; Supplemental Figure S1A). In metaphase cells, nuclear Bik1 was primarily found between SPBs and overlapping with kinetochores. This bilobed kinetochore-associated distribution has also been reported for the kinesins Cin8, Kip1, and Kip3 (Gardner *et al.*, 2008; Tytell and Sorger, 2006; Wargacki *et al.*, 2010). Anaphase cells, on the other hand, displayed nuclear Bik1 concentrated in patches along interpolar microtubules, again similar to what is reported for kinesins Cin8, Kip1, and Kip3. Cytoplasmic Bik1, meanwhile, was localized to astral microtubule tips at the cell cortex.

We then quantified the amount of Bik1 colocalized with kinetochores at different cell cycle stages in cells expressing Bik1-sfGFP and Ndc80-TagRFP-T (kinetochore marker; Figure 1A). We synchronized the cells in G1 using α-factor and subsequently released them in fresh media. We collected samples every 10 min and fixed them in formaldehyde for microscopy. We then measured the amount of Bik1-sfGFP in a region of interest defined by Ndc80-TagRFP-T fluorescence of cells at different cell cycle stages (Figure 1A). We found that Bik1 levels at kinetochores peaked during metaphase, were greatly reduced after anaphase onset (to about 20% of metaphase levels), and remained low in late anaphase and telophase. In interphase cells, Bik1 again colocalized with kinetochores, with concentrations around 50% of those in metaphase cells. Taken together, we conclude that Bik1 localizes to kinetochores in a cell cycle–dependent manner.

To confirm the metaphase colocalization with kinetochores, we used cells expressing the APC/C coactivator Cdc20 under the control of the galactose–inducible *GAL1* promoter. Shifting the carbon source from galactose to glucose represses the expression of *CDC20* and thus arrests the cells at the metaphase-to-anaphase transition. Bik1-sfGFP was localized at kinetochore clusters in metaphase-arrested cells (Figure 1B), confirming what we observed in cycling cells with short spindles. In summary, we conclude that Bik1 colocalizes with kinetochores from G1 until metaphase, after which it instead is localized to interpolar microtubules.

Nuclear Bik1 is needed for timely cell cycle progression

Bik1 in the cytoplasm localizes to astral microtubules and plays an important role in mitotic spindle positioning (Carvalho *et al.*, 2004; Moore *et al.*, 2006). To disrupt the kinetochore function of Bik1 while maintaining its cytoplasmic function, we fused a strong nuclear export consensus sequence (NES; Kosugi *et al.*, 2008) to the C-terminal end of Bik1-sfGFP or Bik1-5xFlag (collectively referred to as Bik1-NES; Figure 1C). We imaged Bik1-NES cells expressing mTurquoise-Tub1 and Nc80-TagRFP-T and confirmed that the mutant indeed excludes Bik1 from the nucleus while maintaining its localization at astral microtubules (Figure 1D). To quantify the effectiveness of the NES, we followed the localization of Bik1 in Bik1-sfGFP and Bik1-sfGFP-NES cells expressing mTurquoise-Tub1. We synchronized the cells in G1 with α-factor, released them in fresh media, and fixed cells at 10-min intervals from release. We then measured Bik1 intensity along the spindle in metaphase cells and found that, as expected, Bik1-NES cells have significantly less sfGFP signal at the spindle microtubules than Bik1 cells (Figure 1E). This was further confirmed by visualizing the nuclei of Bik1-NES expressing cells using the DNA dye Hoechst 33342 (Figure S1B).

We next assessed cell-cycle progression during the release from G1 arrest in the presence and absence of nuclear Bik1. We determined the budding index, which reports the percentage of cells in

the budding phase (S-G2/M) and observed Bik1 and Bik1-NES exit the G1 arrest with similar kinetics (Figure 2A, left graph). Then we scored the number of cells in G1/S, metaphase, or anaphase according to the spindle length (mRuby2-Tub1; Figure 2A, middle and right graphs). The strain expressing Bik1-sfGFP had a sharp peak of metaphase cells at 40 min and a large number of cells with long spindles 50–60 min after the release. Bik1-sfGFP-NES, in contrast, had a shallower slope and a broader metaphase peak that spans between 40 and 60 min postrelease, indicating that cells have a slight delay in entering and exiting metaphase. Bik1-sfGFP-NES cells had a 10-min delay in the anaphase peak, consistent with the metaphase delay.

We then examined Bik1-sfGFP and Bik1-sfGFP-NES cells after G1 synchronization with α-factor by time-lapse imaging (Figure 2, B–E). In the Bik1-sfGFP strain, Bik1 was localized to the kinetochores from G1 through metaphase. When the spindle elongates in anaphase, Bik1 was no longer colocalized with Ndc80 and was found in patches along the interpolar microtubules instead (Figure 2, B and C), as observed in fixed cells (Supplemental Figure S1A). The fluorescence intensity of Bik1-sfGFP at kinetochores was highest at metaphase when kinetochores clustered and reduced to near-background levels in anaphase (Figure 2D). In agreement with the cell-cycle analysis of fixed cells, we observed a slight delay in cell-cycle progression in Bik1-NES cells (Figure 2B, arrows). Our quantifications showed that the time from the appearance of two kinetochore clusters to their separation is approximately 10 min longer in Bik1-NES cells (Figure 2E). Interestingly, we occasionally (in approximately 10% of the cells) observed short spindles transiently transferred into the daughter cell in the Bik1-NES mutant strain before elongation occurred (Figure 2B, 15 min and 25–30 min). This phenomenon could either be an effect of the metaphase delay or, more likely, be due to extra Bik1 (and potential dynein activity) on the astral microtubules in Bik1-NES cells.

Cells lacking nuclear Bik1 display aberrant kinetochore positioning

Because Bik1 colocalizes with kinetochores in metaphase, we hypothesized that the prolonged metaphase of Bik1-NES cells might be due to dysregulation in kinetochore clustering. Indeed, we occasionally observed abnormal, elongated Ndc80 clusters in Bik1-NES cells with short spindles (~1.5 μm inter-SPB distance; Supplemental Figure S2). To quantify the frequency of cells with unclustered kinetochores, we arrested the cells in metaphase (PGal1-Cdc20) and analyzed the distribution of Ndc80-sfGFP relative to the SPBs (Spc42-TagRFP-T) in cells expressing either Bik1-5xFlag or Bik1-5xFlag-NES (Figure 3). While Bik1-5xFlag cells showed separated Ndc80 clusters, we observed cells with long stretches of Ndc80 in the Bik1-5xFlag-NES mutant (Figures 3, A and B). The unclustered kinetochore phenotype was observed in 60% of the Bik1-NES metaphase cells (Figure 3C). Line-scan analysis of the Ndc80-sfGFP fluorescence relative to the SPBs showed that Bik1-NES cells have a flattened distribution of Ndc80 with kinetochores mispositioned toward the spindle equator (Figure 3D).

Bik1 has previously been suggested to contribute to the kinetochore–microtubule attachment. Bik1 is needed to nucleate microtubules that capture kinetochores after centromere reactivation (Tanaka *et al.*, 2005). Furthermore, a binding partner of Bik1, the +TIP Bim1, was recently shown to promote in vitro oligomerization of Dam1 complexes—a major component of the yeast outer kinetochore (Dudziak *et al.*, 2021). Therefore, Bik1's function in kinetochore end-on attachment could contribute to the cell-cycle delay we observe. Yet we did not detect unattached kinetochores in the Bik1-NES mutant. Instead, the kinetochores are aligned in the spindle but appear unclustered during metaphase.

Previous studies have shown that the kinesins Cin8 and to a lesser extent Kip1 and Kip3 are required for yeast chromosome congression (Tytell and Sorger, 2006; Gardner *et al.*, 2008; Wargacki *et al.*, 2010). However, the deletion of each kinesin results in slightly different types of clustering defects. In the cin8Δ mutant, the kinetochores are positioned closer to the spindle equator (Tytell and Sorger, 2006; Gardner *et al.*, 2008; Wargacki *et al.*, 2010). The kip1Δ mutant has a similar, but weaker, phenotype (Tytell and Sorger, 2006; Gardner *et al.*, 2008). Conversely, Ndc80 clusters in kip3Δ cells appear closer to the spindle poles (Wargacki *et al.*, 2010). We found that the Ndc80 foci in the Bik1-NES mutant appear shifted toward the spindle equator (Figure 3D), as has been reported for cin8Δ cells.

Bik1 interacts with Cin8 at the spindle

To investigate Bik1's association with kinesins, we performed single-step affinity purification of Bik1-Flag in metaphase arrested cells, followed by mass spectrometry analysis. Bik1-Flag copurified with the yeast kinesins Kip2, Cin8, Kip1, Kip3, and Kar3 (Table 1). Notably, the kinesins Cin8 and Kip1 had coverage similar to that of the known Bik1-interactor Kip2 (Supplemental Data S1).

The defect of Bik1-NES cells in kinetochore clustering shown in Figure 3A phenocopies *CIN8* and *KIP1* deletions (Tytell and Sorger, 2006; Gardner *et al.*, 2008; Wargacki *et al.*, 2010). Therefore, we decided to study the Bik1-Cin8/Kip1 interactions in more detail. We investigated whether Cin8 and Kip1 interact with Bik1 in vivo using proximity-dependent biotin identification (TurboID), a proximity labeling assay with a labeling radius of about 10 nm from the tag (Kim *et al.*, 2014), that detects both direct and indirect interactions. An advantage of BioID is that it allows detection of weak and transient interactions (Roux *et al.*, 2012). We fused TurboID, a mutated version of a bacterial biotin ligase BirA (Branon *et al.*, 2018; Larochelle *et al.*, 2019), to the C-terminus of Bik1 (Figure 4A). We then Flag-tagged Cin8, Kip1, or Kip2, a kinesin that interacts with Bik1 at astral microtubules (Carvalho *et al.*, 2004). We used the nuclear protein Mre11 as a negative control, as it is not expected to interact with Bik1, while having a nuclear localization. Cin8, Kip1, and Kip2 were recovered after streptavidin pulldown when expressed in Bik1-TurboID cells, indicating that Bik1 is in close proximity to Cin8 and Kip1 in vivo (Figure 4B and Supplemental Figure S3). Because of cin8Δ's reportedly stronger phenotype, we continued to study the Bik1/Cin8 interaction in further detail.

We next looked at the interaction between Bik1 and Cin8 in individual cells by bimolecular fluorescence complementation (BiFC; Sung and Huh, 2007). Briefly, an N-terminal fragment of the yellow fluorescent protein Venus was fused to the C-terminus of Bik1, and a complementary C-terminal Venus fragment was fused to the C-terminus of Cin8. We detected BiFC signals at the spindle, predominantly in metaphase and anaphase cells (Figure 4, C and D). Interestingly, the BiFC signal in metaphase cells appeared as one or two dots at the spindle, while the signal in anaphase cells appeared as a single dot around the spindle midzone (Figure 4C). Cin8 is localized to interpolar microtubules and specifically to the midzone in anaphase, where it drives spindle elongation (Goldstein *et al.*, 2017; Suzuki *et al.*, 2018). It is possible that Bik1 interacts with Cin8 there as well, although we cannot exclude the possibility that this is caused by the irreversible binding of the BiFC complexes (Shyu and Hu, 2008).

We then investigated the dependence of Cin8 and Bik1 for localizing to the spindle. In the Bik1-NES mutant, Cin8 still forms two foci between SPBs and kinetochores (Figure 5, A and B), even in cells

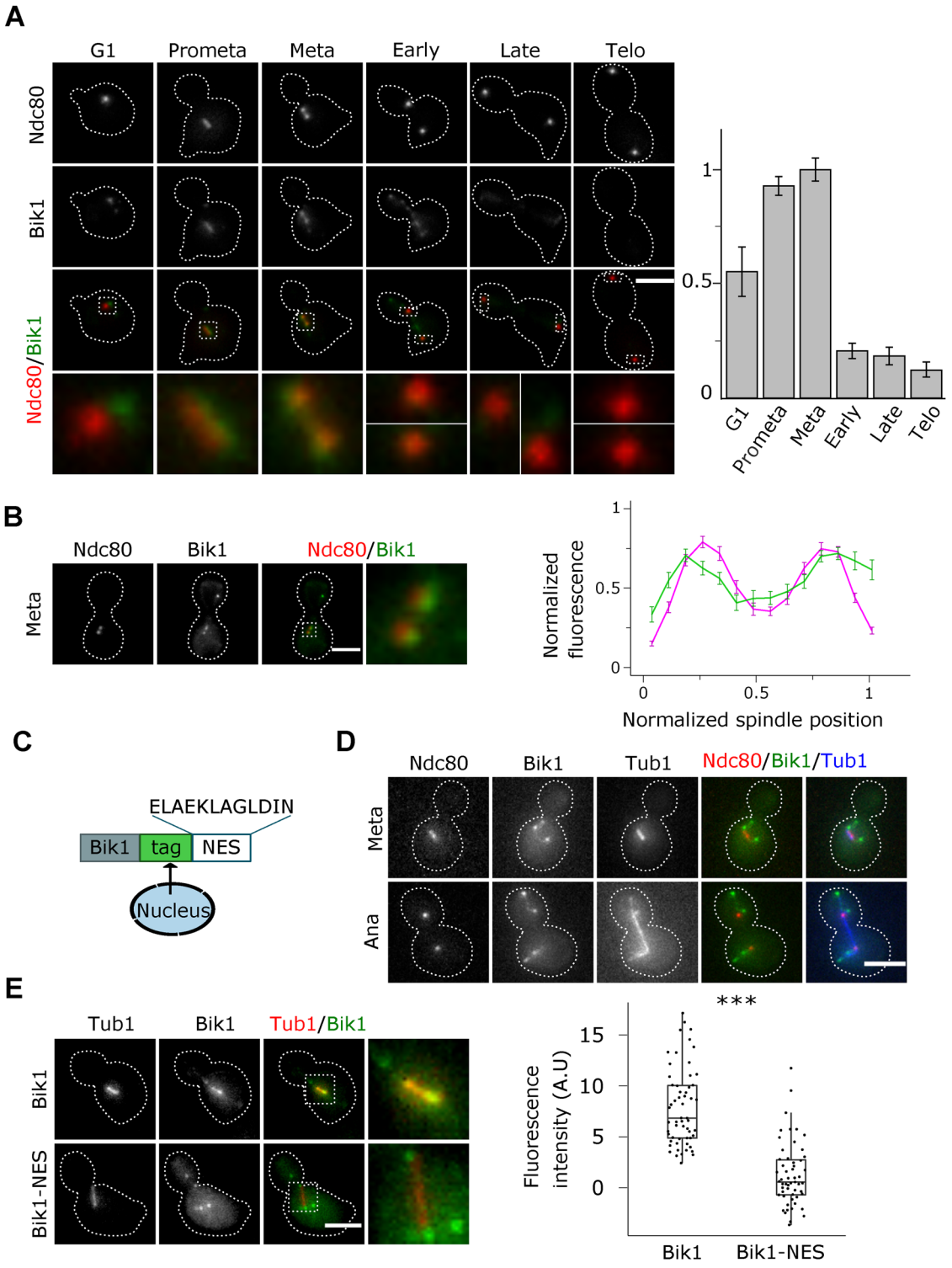

FIGURE 1: Bik1 localizes to kinetochores in a cell cycle–dependent manner. (A) Left panel: representative images of Bik1-sfGFP (green) localization at different cell cycle stages. Cells expressing Ndc80-TagRFP-T (red) and Bik1-sfGFP (green) were synchronized in G1 using α factor and then released in fresh media and fixed at 10-min intervals. Cell-cycle stages were determined using Ndc80 morphology and bud size. Images are maximum intensity projections of *z*-stacks (6.3 µm, 0.3-µm steps). Right panel: Bik1 fluorescence levels were measured at kinetochores and normalized to metaphase levels. Error bars represent mean ± sd ($n = 3$ independent experiments, with 50-57 cells analyzed in each cell cycle phase per experiment). (B) Left panel: representative images of Bik1-sfGFP (green) localization in pGal1-Cdc20 metaphase-arrested cells expressing Nc80-TagRFP-T. Right panel: line-scan analysis shows the distribution of Bik1-sfGFP and kinetochores (Ndc80-TagRFP-T) in metaphase-arrested cells. For each cell, the fluorescence intensity was measured along a line drawn between the kinetochore foci and normalized relative to the maximum value, and the mean values ± SEM (standard error of the mean) are shown ($n = 26$ cells). (C) Cartoon showing the design of Bik1-NES. In short, a strong nuclear export signal (NES) was fused to Bik1-sfGFP or Bik1 5xFlag to promote nuclear export.

with unclustered kinetochores. This result was surprising, as Cin8 has been shown to bind kinetochores directly (Suzuki *et al.*, 2018). Line-scan analysis of Cin8-sfGFP localization in relation to SPBs showed that Cin8 localization is unaltered in the absence of nuclear Bik1 (Figure 5B). Deletion of CIN8, on the other hand, resulted in a significantly reduced Bik1 intensity at the spindle (Figure 5, C and D). Overall, these data suggest that nuclear Bik1 partially depends on Cin8 to bind the spindle. Kinetochores might have other adaptors for Bik1, in addition to Cin8. Indeed, the BioID experiments showed that the nuclear kinesin Kip1 also is also proximity interactors of Bik1. Kip1 and Cin8 both affect chromosome congression (Gardner *et al.*, 2008; Tytell and Sorger, 2006) and have at least partially redundant functionality (Costanzo *et al.*, 2016; Tong *et al.*, 2004). It is therefore possible that Kip1 also affects Bik1's binding to the spindle and colocalization with kinetochores.

The reduced Bik1 recruitment to the spindle and kinetochores in the cin8Δ mutant could explain, at least in part, why Bik1 cannot compensate for the lack of Cin8, which is known to cause severe defects in assembling the mitotic spindle (Hoyt *et al.*, 1992; Kotwaliwale *et al.*, 2007). A previous study has shown that Cin8 mediates chromosome congression by depolymerizing kinetochore microtubules in a length-dependent manner (Gardner *et al.*, 2008). Gardner and coworkers proposed that Cin8 binds randomly to kinetochore microtubules and walks toward the plus-end to promote microtubule plus-end disassembly directly. However, in Bik1-NES cells, Cin8 is insufficient to regulate chromosome congression. Moreover, Cin8 does not localize to the unclustered kinetochores in the Bik1-NES mutant. Taken together, these observations suggest that Bik1 is a binding partner of Cin8 that contributes to the disassembly of kinetochore microtubules to achieve chromosome congression at metaphase. There are at least two other examples where plus-end directed kinesin motors interact with Bik1. Kip2 transports Bik1 to astral microtubule plus ends to ensure proper spindle alignment (Carvalho *et al.*, 2004; Caudron *et al.*, 2008). Furthermore, it has been suggested that Bik1 and Kar3 form a complex at the junction of oppositely oriented MTs during mating to induce microtubule depolymerization for nuclear congression to occur (Molk *et al.*, 2006).

We propose that Bik1 increases the processivity of Cin8. Bik1 has been suggested to be a processivity factor for the kinesin Kip2 at astral microtubules (Hibbel *et al.*, 2015). Likewise, Bik1 might contribute to Cin8 reaching the plus-ends of long kinetochore microtubules that extend beyond bundled kinetochore microtubules. Dysregulation of these long KT-MTs would then result in the unclustered phenotype observed in the Bik1-NES mutant. Cin8 is a bidirectional kinesin and in vitro studies have shown that it preferentially moves in a minus end–directed manner as single motors (Gerson-Gurwitz *et al.*, 2011; Pandey *et al.*, 2021; Roostalu *et al.*, 2011). Directional switching occurs when Cin8 motors are clustered (Pandey *et al.*, 2021; Roostalu *et al.*, 2011), and other kinesin-5 motors switch directionality in response to steric crowding on MTs (Britto *et al.*, 2016). Loss of nuclear Bik1 could therefore lead to ineffective plus end–directed movement of Cin8 on long kinetochore microtubules and failure to cluster kinetochores at metaphase. This is supported by the observation that Cin8 is not localized along the rodlike distribution of Ndc80 in the Bik1-NES mutant.

MATERIALS AND METHODS

Request a protocol through *Bio-protocol*.

Yeast strains and plasmids

All *S. cerevisiae* strains used in this study were derivatives of BY4741 and are listed in Supplemental Table S1. The epitope-tagged alleles (sfGFP and TagRFP-T), TurboID-3xmyc, and BiFC were constructed at the endogenous loci by standard PCR-based integration as described in Longtine *et al.* (1998) and confirmed by PCR, sequencing, and microscopy. The plasmids used to generate the strains are listed in Supplemental Table S2. Strains with fluorescently tagged Tub1 were constructed as described in Markus *et al.* (2015). Briefly, the listed plasmids were linearized using BsaBI (New England Biolabs, R0537S) and integrated at the endogenous TUB1 locus by homologous recombination.

Growth conditions

Cells were grown at 30°C in YEP (1% yeast extract, 2% bactopeptone) medium supplemented with 2% glucose (YEPD) unless otherwise stated. For G1 arrest, overnight cultures were diluted to $OD_{600} = 0.1$ in fresh media, grown for 2.5 h, and arrested by adding 3 µg/ml α-factor (Sigma, custom peptide WHWLQLKPGQPMY) every 60 min for 120 min. Cells were released by washing away α-factor with 1× culture volume of YEPD and resuspending in 1× culture volume of YEPD and further grown at 30°C. For metaphase arrest, PGal1-Cdc20 cells were grown in YEP supplemented with 2% raffinose and 2% galactose and switched to YEPD for 120 min.

Fluorescence imaging

Cells were fixed in 4% formaldehyde on ice for 60 min, washed with phosphate-buffered saline (PBS), and stored in PBS at 4°C until imaging. DNA staining was done by incubating fixed cells with Hoechst-33342 (ThermoFisher Scientific, H1399) diluted 1:10,000 in PBS for 30 min before imaging. Cells were imaged in concanavalin A-coated 96-well glass-bottomed plates. Images were acquired using a Nikon Ti microscope equipped with a Zyla 4.2+ sCMOS camera and a 60× water immersion objective (NA 1.2). *z*-stack images were captured for fixed cells, as described in the figure legends. Images for BiFC and immunofluorescence were acquired using a Nikon Ti2 microscope equipped with a Prime BSI sCMOS camera and a 60× water immersion objective (NA 1.2).

(D) Representative images of Bik1-sfGFP-NES (green) localization in cycling cells expressing mTurquoise-Tub1 (blue) and Ndc80-TagRFP-T (red). (E) Quantification of Bik1-sfGFP or Bik1-sfGFP-NES localization in metaphase cells. Bik1-sfGFP and Bik1-sfGFP-NES cells expressing mRuby2-Tub1 were arrested in G1 with α-factor and subsequently released in fresh media. Cells were fixed every 10 min for 120 min. Left: representative cells at metaphase. Time after release = 40 min (Bik1-sfGFP) and 50 min (Bik1-sfGFP-NES). Right: boxplots of the integrated fluorescence intensity of Bik1-sfGFP and Bik1-sfGFP-NES at the spindle (mRuby2-Tub1) in metaphase cells. Dots represent individual measured values. Boxes correspond to the 25th and 75th percentiles of values. The horizontal lines within the boxes represent the median. Whiskers extend to the largest/smallest value within 1.5× interquartile range, $n = 59$ cells for Bik1-sfGFP and 55 for Bik1-sfGFP-NES, p-value = 2.2×10^{-16} using Welch two-sample t-test (two-sided). All images are maximum-intensity projections of *z*-stacks (9 µm, 1-µm steps) unless otherwise stated. Dashed boxes show areas enlarged in the uppermost, A, or rightmost, B and E, images. Dashed lines represent the cell outlines based on bright field images. All scale bars 4 µm.

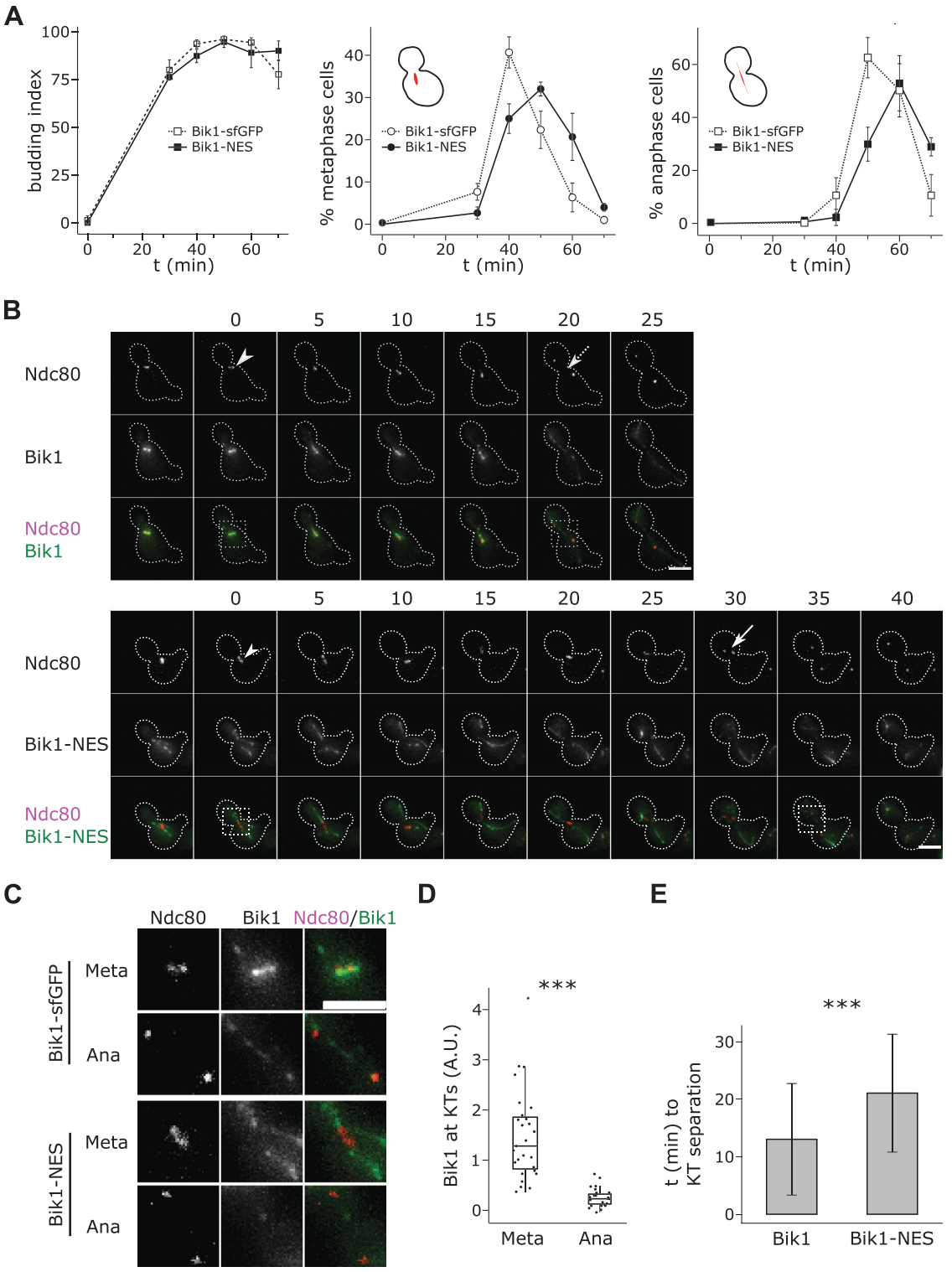

FIGURE 2: Bik1-NES delays spindle elongation at metaphase/anaphase transition. (A) Cells from 1E were scored for cell-cycle progression based on the budding index (left) and bud size and spindle length (mRuby-Tub1; middle and right). Error bars represent mean ± sd ($n = 3$ independent experiments, 100 cells each timepoint for each strain analyzed per experiment). (B–E) Time-lapse imaging of cells expressing Bik1-sfGFP or Bik1-sfGFP-NES (green) and Ndc80-TagRFP-T (red). Cells were arrested in G1 with α-factor and subsequently released in fresh medium under the microscope. Images were taken at 5-min intervals. (B) Representative time-lapse images. Arrowheads indicate the appearance of bilobed kinetochore clusters. Arrows indicate the appearance of separated kinetochores. The time (min) elapsed from the appearance of bilobed kinetochore clusters is indicated by the numbers above the frames. Dashed boxes show area enlarged in C. Images are maximum-intensity projections of *z*-stacks (9 μm, 1-μm steps). Scale bar 4 μm. (C) Zoomed-in images from the dashed areas of B showing the kinetochores (Ndc80-TagRFP-T) at metaphase and anaphase. (D) Boxplots of the integrated Bik1-sfGFP fluorescence intensity at kinetochores (Ndc80-TagRFP-T) at

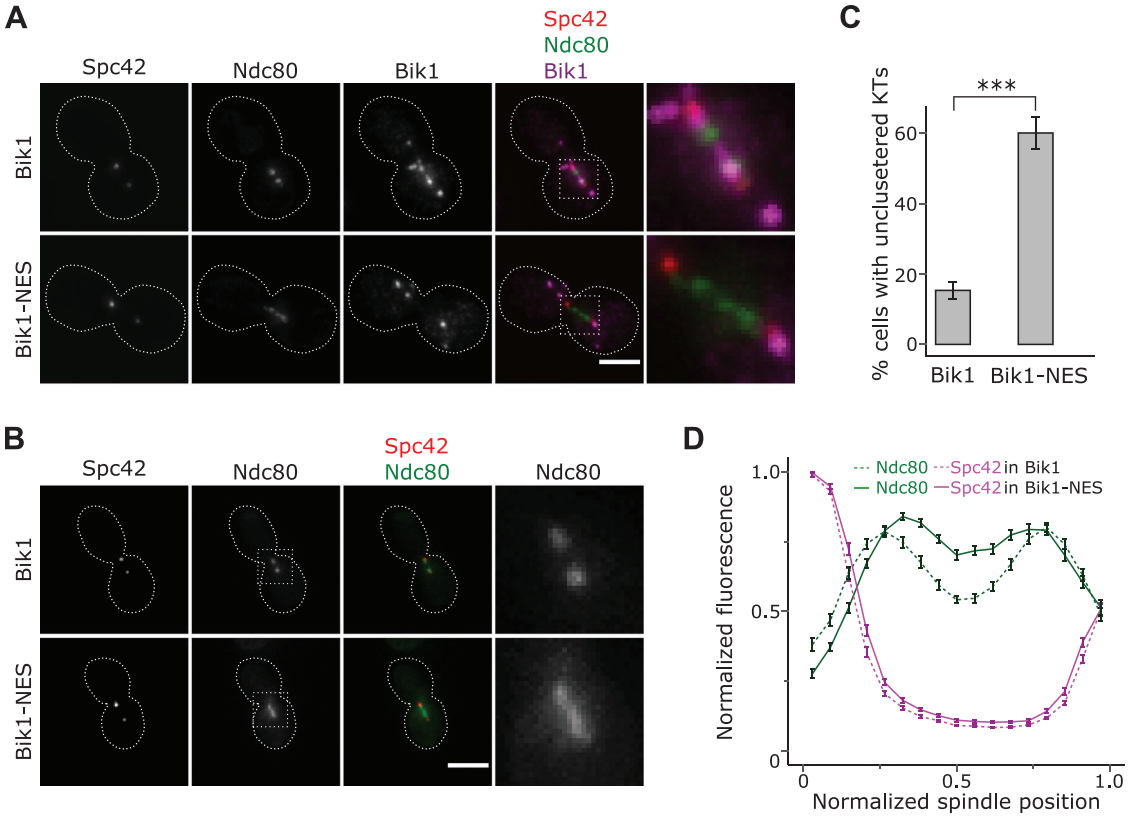

FIGURE 3: Nuclear Bik1 is needed for kinetochore clustering at metaphase. (A) Representative immunofluorescence staining for Bik1-5xFlag and Bik1-5xFlag-NES (magenta) in metaphase-arrested pGal1-Cdc20 cells expressing Spc42-TagRFP-T (red) and Ndc80-sfGFP (green). Images are maximum-intensity projections of *z*-stacks (4.95 µm, 0.3-µm steps). Dashed boxes show area enlarged in the rightmost images. Scale bar 4 µm. (B) Representative images of Bik1-5xFlag and Bik1-5xFlag-NES arrested as in A, including zoomed-in images of the kinetochores (Ndc80-sfGFP). Images are maximum-intensity projections of *z*-stacks (8.7 µm, 0.3-µm steps). Dashed boxes show area enlarged in the rightmost image. Scale bar 4 µm. (C) Quantification of kinetochore (Ndc80-sfGFP) unclustered phenotype in Bik1-5xFlag and Bik-5xFlag-NES cells arrested in metaphase as shown in B. Error bars represent mean ± sd, $n = 3$ independent experiments, with 100 cells for each strain. *p*-value = 0.0006884 using Welch two-sample *t* test (two-sided). (D) Line-scan analysis shows the distribution of kinetochores (Ndc80-sfGFP) and spindle pole bodies (SPBs, Spc42-TagRFP-T) in metaphase-arrested cells. For each cell, the fluorescence intensity was measured along lines drawn between the SPBs (Spc42-TagRFP-T) and normalized relative to the maximum value. Mean values ± SEM, $n = 100$ cells for each strain.

Live-cell imaging

Cells were arrested in G1 with as α-factor and subsequently released in low-fluorescence media (LFM) containing 1.7 g/l yeast nitrogen base without ammonium sulfate, amino acids, folic acid, and riboflavin (MP-Biomedicals, 4030-512), and 1 g/l monosodium glutamate, supplemented with 2% glucose and amino acids. Cells were left to settle on the bottom of concanavalin A-coated 96-well glass-bottomed plates for 20–30 min inside the microscope incubator at 30°C before being imaged. Images were captured every 5 min for 100–120 min.

Image analysis

Fluorescence intensity measurements were made from maximum-intensity projections of image *z*-stacks using FiJi (Schindelin *et al.*, 2012). Integrated intensities were measured in a region of interest drawn around spindles/kinetochores. Background correction was done by multiplying the mean fluorescence of regions outside of the nucleus by the measured region's area and subtracting from the measured integrated intensity. Line-scan analysis was performed by drawing a line between the centers of opposing SPB foci (from the brighter SPB toward the dimmer SPB) and measuring the fluorescence intensities along the line. For the line scans with Ndc80 we draw the line from the Ndc80 closer to the bud. Background correction was done by subtracting the mean fluorescence measured at the cytoplasm. Binned means were calculated for each strain. Cell cycle analyses were performed by classifying the cells according to the spindle length, based on the Tub1-TagRFP-T marker: (G1/S) spindles <1 µm, metaphase 1–2 µm, and anaphase >2 µm.

metaphase (meta) and anaphase (ana). Dots represent individual measured values. Boxes correspond to the 25th and 75th percentiles of values. The horizontal lines within the boxes represent the median. Whiskers extend to largest/smallest value within 1.5× interquartile range. $n = 27$ cells per strain, *p*-value = 1.33×10^{-7} using Welch two-sample *t*-test (two-sided). (E) Quantification of average time from the appearance of bilobed kinetochore clusters to separated kinetochores in Bik1-sfGFP and Bik1-sfGFP-NES cells. We performed two independent experiments and pooled the data. Error bars represent mean ± sd, $n = 59$ cells for Bik1-sfGFP and 57 for Bik1-sfGFP-NES, *p*-value = 6.097×10^{-6} using the Mann–Whitney test.

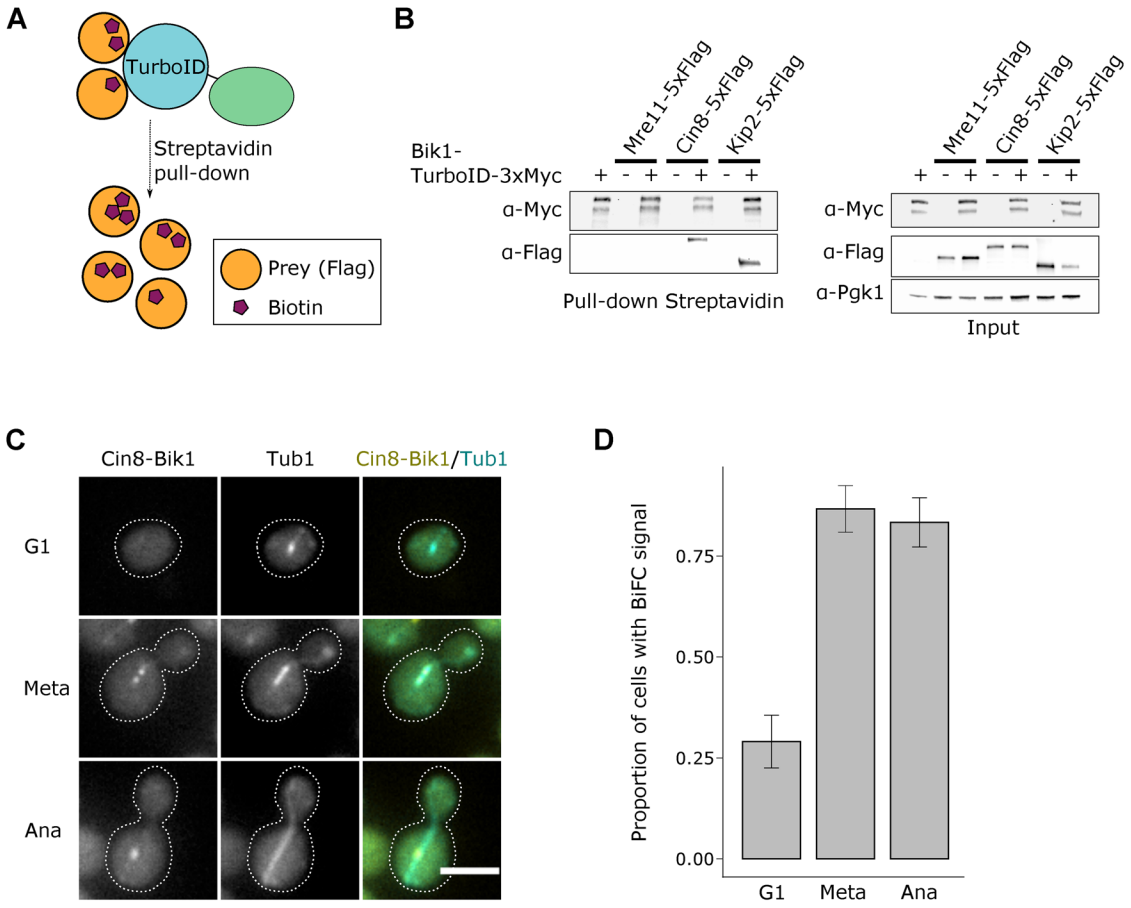

FIGURE 4: Bik1 interacts with Cin8 at metaphase. (A, B) Identification of Cin8 as a Bik1 interaction partner using TurboID. Cartoon outlining the principle of the TurboID assay. Briefly, a biotin ligase was fused to endogenous Bik1 (Bik1-TurboID) in cells expressing the protein of interest tagged with Flag (Prey). Biotinylated substrates were purified using streptavidin beads, and inputs and pull-down lysates were analyzed by immunoblot for the indicated proteins. (B) Western blot analysis of total cell extracts (input) and streptavidin pull-downs prepared from Bik1-TurboID-3xmyc cells expressing Mre11-5xFlag, Cin8-5xFlag, or Kip2-5xFlag as prey, and control strains, using anti-Myc (top) and anti-Flag (bottom) antibodies. (C, D) Bimolecular fluorescence complementation (BiFC) analysis of Bik1 and Cin8 interaction. C, representative images of cycling cells expressing Bik1-VN and Cin8-VC in G1, metaphase and anaphase. Images shown are single focal planes. D, proportion of cells in C with BIFC signal based on Venus fluorescence. Error bars represent mean ± sd (n = 3 independent experiments, with 50 cells analyzed in each cell cycle phase per experiment).

Immunofluorescence

PGal1-Cdc20 cells were arrested in metaphase and fixed by adding formaldehyde to 3.7% (vol/vol) and incubating while shaking at 30°C for 30 min. The fixed cells were washed once with PBS and then twice with SP buffer (0.1 M KPO_4, 1.2 M sorbitol, pH 7.5). The cells were resuspended in 500 µl SP buffer with 0.1% β-mercaptoethanol and 10 µl of 20 mg/ml Zymoylase-20T (Seikagaku). The cells were incubated with soft rotation for 20 min at room temperature (RT). The resulting spheroplasts were then washed twice in SP buffer and permeabilized in blocking solution (3% bovine serum albumin, 0.1% Triton X-100 in PBS) for 30 min at RT. The spheroplasts were immunostained in suspension. First, cells were incubated with 1:1000 mouse monoclonal anti-FLAG M2 antibody (Sigma, F1804) in blocking buffer for 1 h at RT. Cells were washed three times in PBS and then incubated with 1:100 donkey anti-mouse Alexa Fluor 647 antibody (ThermoFisher, A-31571) for 45 min at RT. Cells were washed three times in PBS, seeded in a glass-bottomed imaging plate coated with Concanavalin A, and imaged.

Sample preparation for mass spectrometry analysis

Bik1-5xFlag PGal1-Cdc20 cells were arrested in metaphase. Briefly, cells were grown overnight in 50 ml YEP with 2% galactose and 2% raffinose. Cells were diluted in 2 l YEP with 2% galactose and 2% raffinose and grown at 30°C to OD_{600} = 1. Then, cells were spun down and resuspended in 2 l YEPD with 2% glucose and arrested at 30°C for 2 h. Cells were spun down at 6000 rpm at 4°C, washed with cold dH_2O, and spun down at 6000 rpm at 4°C. The cell pellet was diluted in a few drops of lysis buffer (50 mM Tris, pH 8.0, 150 mM NaCl, 5% glycerol, 0.1% Triton X-100). The cell suspension was snap-frozen by pipetting the drops directly into liquid nitrogen. The frozen pellets were then lysed using a Freezer/Mill (SPEX sample prep freezer/mill), using 10 rounds consisting of 2 min grinding at 14 cps (counts per second), 2 min cooling. The yeast pellets were diluted in buffer EB1 (40 mM sodium hepes, 300 mM NaCl, 0.5% Triton X-100, 2 mM $MgCl_2$, 5% glycerol and protease and phosphatase inhibitors [1 mM PMSF, 1 mM leupeptin, 1 mM peptasin A, 10 mM NaF, 1 mM sodium pyrophosphatase, 1 mm sodium orthovanadate]), and clarified by centrifugation at 10,000 × g for

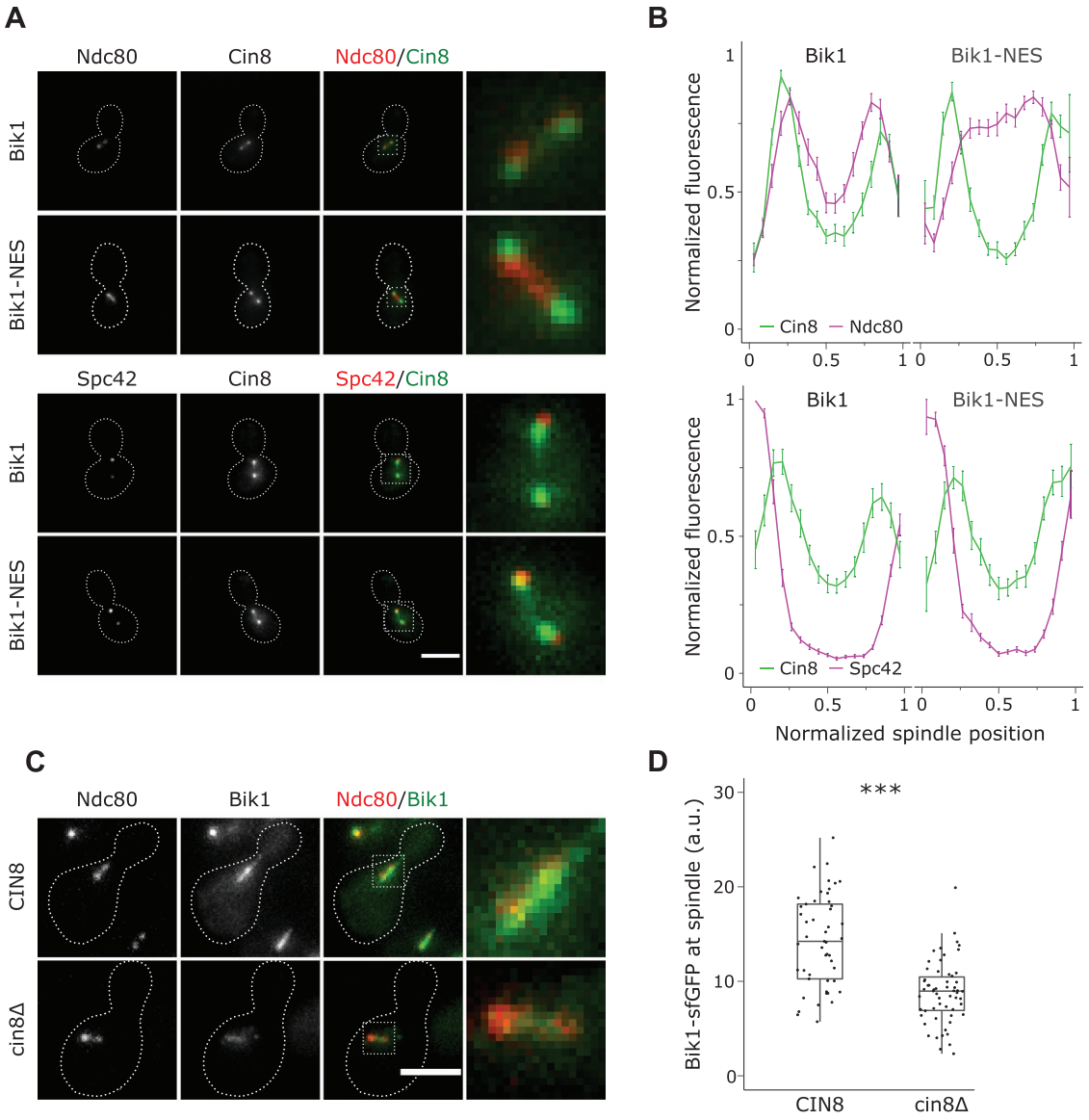

FIGURE 5: Dependence of Cin8 and Bik1 to localize to the spindle. (A, B) Cin8 localizes at the spindle in Bik1-NES cells but does not colocalize with unclustered kinetochores. A, Cin8 localization at the metaphase spindle does not require nuclear Bik1. Representative images of pGal1-Cdc20 cells arrested in metaphase expressing Bik1-5xFlag or Bik1-5xFlag-NES, Cin8-sfGFP, and the markers Ndc80-TagRFP-T (top panel) or Spc42-TagRFP-T (lower panel). Images shown are maximum-intensity projections of *z*-stacks (8.7 µm, 0.3-µm steps). Dashed boxes show area enlarged in the rightmost images. Scale bar 4 µm. B, line-scan analysis of Cin8 distribution (Cin8-sfGFP) in metaphase-arrested cells. Top panel: Cin8 distribution relative to the kinetochores (Ndc80-TagRFP-T). For each cell, the fluorescence intensities of Cin8-sfGFP and Ndc80-TagRFP-T was measured along lines drawn between the SPBs and normalized relative to the maximum values, mean values ± SEM are shown ($n = 25$ cells for BIK1 and 25 for Bik1-5xFlag-NES). Bottom panel: Cin8 distribution relative to the SPBs (Spc42-TagRFP-T). For each cell, the fluorescence intensity of Cin8-sfGFP and Spc42-TagRFP-T was measured along a line drawn between the SPBs and normalized relative to the maximum value. Mean values ± SEM are shown ($n = 25$ cells for Bik1-5xFlag and 26 for Bik1-5xFlag-NES). (C) Cin8 is needed for Bik1-sfGFP localization at kinetochores. CIN8 and cin8Δ cells expressing Bik1-sfGFP and Ndc80-TagRFP-T were arrested in G1 using α-factor, released in fresh media at 25°C, and fixed every 10 min for 130 min. Left: representative images of cells in metaphase (CIN8, 60 min after release; cin8Δ, 110 min after release). Images shown are maximum intensity projections of *z*-stacks (6.6 µm, 0.6-µm steps). Dashed boxes show area enlarged in the rightmost images. Scale bar, 4 µm. (D) Boxplots of the integrated fluorescence intensity of Bik1-sfGFP at the spindle (based on Ndc80-TagRFP-T localization) in metaphase cells ($n = 100$ cells for each strain (CIN8 and cin8 Δ). Dots represent individual measured values. Boxes correspond to the 25th and 75th percentiles of values. The horizontal lines within the boxes represent the median. Whiskers extend to largest/smallest value within 1.5× interquartile range. *p*-value = 0.0001156 using Welch two-sample *t*-test (two-sided).

10 min at 4°C. The cleared lysate was incubated for 30 min with magnetic Dynabeads (Thermo Fisher Scientific) coupled with anti-FLAG M2 antibody (Sigma-Aldrich). The Dynabeads were washed three times with buffer A (25 mM sodium HEPES, 2 mM $MgCl_2$, 0.1% EDTA, 0.1% Triton X-100, 5% glycerol, 150 mM NaCl, protease and phosphatase inhibitors [1 mM PMSF, 1 mM leupeptin, 1 mM

peptasin A, 10 mM NaF, 1 mM sodium pyrophosphatase, 1 mm sodium orthovanadate]) and four times with buffer B (25 mM HEPES, pH 8.0, and 150 mM KCl).

Protein on-beads digestion

Proteins bound to the Dynabeads were resuspended and washed twice with 500 µl of 50 mM ammonium bicarbonate (AmBic), pH 8.0. After incubation at room temperature for 15 min, 50 µl of 50 mM AmBic was added. Protein disulfide bonds were reduced with 5 µl of 200 mM dithiothreitol at 37°C for 45 min and alkylated with 5 µl of 600 mM iodoacetamide at room temperature in dark for 30 min. Tryptic digestion was started by adding 1 µg of trypsin and incubation at 37°C overnight, followed by adding another 500 ng of trypsin and incubation at 30°C for 3 h. The digestion was stopped with 5 µl concentrated formic acid. The samples were then cleaned on a C18 StageTip (Thermo Scientific) and dried using a SpeedVac (MiVac, Thermo Scientific).

PRLC-MS/MS analysis

Chromatographic separations of peptides were performed on a 50 cm–long C18 EASY-spray column connected to an Easy nanoLC-1000 UPLC system (Thermo Fisher Scientific). The gradient was 4–25% of solvent B (98% acetonitrile, 0.1% formic acid) for 50 min and 25–40%B for 10 min at a flow rate of 300 nl/min. An Orbitrap Fusion mass spectrometer (Thermo Scientific) analyzed the eluted peptides that were ionized in a nano-Easy electrospray source. The survey mass spectrum was acquired at the resolution of 120,000 in the range of *m/z* 350–1800. MS/MS data of precursors were obtained with 30% normalized collision energy by higher-energy collisional dissociation (HCD) for ions with charge $z = 2–7$ at a resolution of 30,000 in cycle time 3 s.

Data analysis

A Mascot v 2.5.1 search engine (MatrixScience, UK) was used for protein identification with the following search parameters: up to two missed cleavage sites for trypsin, peptide mass tolerance 10 ppm, 0.05 Da for the HCD fragment ions. Carbamidomethylation of cysteine was specified as a fixed modification, whereas oxidation of methionine and deamidation of asparagine and glutamine were defined as variable modifications.

Turbo-ID assay

Overnight cultures were diluted to $OD_{600} = 0.2$ in YEPD medium supplemented with 50 µM biotin and grown at 30°C until they reached $OD_{600} = 0.6$ (4–5 h). Cells were pelleted and resuspended in RIPA buffer (50 mM Tris-HCl, 150 mM NaCl, 1 mM EDTA, 0.1% SDS, 1% Triton X-100, 1.5 mM $MgCl_2$, 0.4% sodium deoxycholate, 1 mM DTT, 1 mM PMSF, 1 mM leupeptin and1 mM pepstatin A). The cells were lysed using acid-washed glass beads and a bead-beater at 4°. To shear the DNA and RNA, the cell lysate was sonicated and then clarified by centrifugation. Clarified lysates were incubated with 100 µl of Streptavidin-Sepharose beads (GE Healthcare; 17-5113-01) for 3 h at 40°C. The beads were then washed once with wash buffer (50 mM Tris-HCl, 2% SDS) and three times with RIPA buffer. The purified proteins were eluted with 4 × Laemmli buffer containing 25 µM biotin and 10% β-mercaptoethanol for 15 min at 95°C. The whole cell extract or pull-down samples were separated by SDS–PAGE, and the proteins were transferred to a PVDF membrane (BioRad) followed by standard immunoblotting. Primary monoclonal anti-FLAG M2 antibody (Sigma-Aldrich, F3165, diluted 1:5000), c-Myc rabbit polyclonal antibody (Santa Cruz Biotechnology, sc-789, diluted 1:5000); and anti-Pgk1 mouse monoclonal antibody (Invitrogen, 45925, diluted 1:5000) and secondary anti-mouse IgG peroxidase antibody (Sigma, A9044, diluted 1:50000) were used. HRP conjugated secondary antibodies were detected with Femto ECL (ThermoFisher Scientific).

ACKNOWLEDGMENTS

We thank C. Björkegren (Karolinska Institutet, Sweden) for reagents and C. Boone and Z. Li for help with construction of deletion mutants and critical reading of this manuscript. Microscopy was performed at the Live Cell Imaging core facility/Nikon Center of Excellence at the Karolinska Institutet, supported by grants from the Swedish Research Council, KI infrastructure, and the Centre for Innovative Medicine. The BioImage Informatics Facility at SciLifeLab, the National Microscopy Infrastructure (VR-RFI 2019-00217), and a recipient of the Chan-Zuckerberg Initiative assisted in the image analysis. Protein identification and quantification were carried out by the Proteomics Biomedicum core facility, Karolinska Institutet. This work was supported by grants from the Swedish Council (VR-NT 2017-04536) and STINT (Mobility Grant for Internationalization, MG2019-8484) to V.M.B.

REFERENCES

Akhmanova A, Steinmetz MO (2010). Microtubule +TIPs at a glance. J Cell Sci 123. https://doi.org/10.1242/jcs.062414

Berlin V, Styles CA, Fink GR (1990). BIK1, a protein required for microtubule function during mating and mitosis in *Saccharomyces cerevisiae*, colocalizes with tubulin. J Cell Biol 111. https://doi.org/10.1083/jcb.111.6.2573

Branon TC, Bosch JA, Sanchez AD, Udeshi ND, Svinkina T, Carr SA, Feldman JL, Perrimon N, Ting AY (2018). Efficient proximity labeling in living cells and organisms with TurboID. Nature Biotechnol 36. https://doi.org/10.1038/nbt.4201

Britto M, Goulet A, Rizvi S, Von Loeffelholz O, Moores CA, Cross RA (2016). *Schizosaccharomyces pombe* kinesin-5 switches direction using a steric blocking mechanism. Proc Natl Acad Sci USA, 113. https://doi.org/10.1073/pnas.1611581113

Carvalho P, Gupta ML, Hoyt MA, Pellman D (2004). Cell cycle control of kinesin-mediated transport of Bik1 (CLIP-170) regulates microtubule stability and dynein activation. Dev Cell 6. https://doi.org/10.1016/j.devcel.2004.05.001

Caudron F, Andrieux A, Job D, Boscheron C (2008). A new role for kinesin-directed transport of Bik1p (CLIP-170) in *Saccharomyces cerevisiae*. J Cell Sci 121. https://doi.org/10.1242/jcs.023374

Costanzo M, VanderSluis B, Koch EN, Baryshnikova A, Pons C, Tan G, Wang W, Usaj M, Hanchard J, Lee SD, *et al.* (2016). A global genetic interaction network maps a wiring diagram of cellular function. Science 353. https://doi.org/10.1126/science.aaf1420

Dudziak A, Engelhard L, Bourque C, Klink BU, Rombaut P, Kornakov N, Jänen K, Herzog F, Gatsogiannis C, Westermann S (2021). Phospho-regulated Bim1/EB1 interactions trigger Dam1c ring assembly at the budding yeast outer kinetochore. EMBO J 40. https://doi.org/10.15252/embj.2021108004

Gardner MK, Bouck DC, Paliulis LV, Meehl JB, O'Toole ET, Haase J, Soubry A, Joglekar AP, Winey M, Salmon ED, *et al.* (2008). Chromosome congression by kKinesin-5 motor-mediated disassembly of longer kinetochore microtubules. Cell 135. https://doi.org/10.1016/j.cell.2008.09.046

Gardner MK, Pearson CG, Sprague BL, Zarzar TR, Bloom K, Salmon ED, Odde DJ (2005). Tension-dependent regulation of microtubule dynamics at kinetochores can explain metaphase congression in yeast. Mol Biol Cell 16, 3764–3775.

Gerson-Gurwitz A, Thiede C, Movshovich N, Fridman V, Podolskaya M, Danieli T, Lakämper S, Klopfenstein DR, Schmidt CF, Gheber L (2011). Directionality of individual kinesin-5 Cin8 motors is modulated by loop 8, ionic strength and microtubule geometry. EMBO J 30. https://doi.org/10.1038/emboj.2011.403

Goldstein A, Siegler N, Goldman D, Judah H, Valk E, Kõivomägi M, Loog M, Gheber L (2017). Three Cdk1 sites in the kinesin-5 Cin8 catalytic

domain coordinate motor localization and activity during anaphase. Cell Mol Life Sci 74. https://doi.org/10.1007/s00018-017-2523-z
Hibbel A, Bogdanova A, Mahamdeh M, Jannasch A, Storch M, Schäffer E, Liakopoulos D, Howard J (2015). Kinesin Kip2 enhances microtubule growth in vitro through length-dependent feedback on polymerization and catastrophe. ELife 4(NOVEMBER2015). https://doi.org/10.7554/eLife.10542
Hoyt MA, He L, Loo KK, Saunders WS. (1992). Two *Saccharomyces cerevisiae* kinesin-related gene products required for mitotic spindle assembly. J Cell Biol 118. https://doi.org/10.1083/jcb.118.1.109
Kim DI, Birendra KC, Zhu W, Motamedchaboki K, Doye V, Roux KJ (2014). Probing nuclear pore complex architecture with proximity-dependent biotinylation. Proc Natl Acad Sci USA 111. https://doi.org/10.1073/pnas.1406459111
Kops GJPL, Saurin AT, Meraldi P (2010). Finding the middle ground: how kinetochores power chromosome congression. In Cell Mol Life Sci 67. https://doi.org/10.1007/s00018-010-0321-y
Kosugi S, Hasebe M, Tomita M, Yanagawa H (2008). Nuclear export signal consensus sequences defined using a localization-based yeast selection system. Traffic 9. https://doi.org/10.1111/j.1600-0854.2008.00825.x
Kotwaliwale CV, Frei SB, Stern BM, Biggins S (2007). A pathway containing the Ipl1/Aurora protein kinase and the spindle midzone protein Ase1 Rregulates yeast spindle assembly. Dev Cell 13. https://doi.org/10.1016/j.devcel.2007.07.003
Larochelle M, Bergeron D, Arcand B, Bachand F (2019). Proximity-dependent biotinylation mediated by TurboID to identify protein-protein interaction networks in yeast. J Cell Sci 132. https://doi.org/10.1242/jcs.232249
Lin H, De Carvalho P, Kho D, Tai CY, Pierre P, Fink GR, Pellman D (2001). Polyploids require Bik1 for kinetochore-microtubule attachment. J Cell Biol 155. https://doi.org/10.1083/jcb.200108119
Longtine MS, McKenzie A 3rd, Demarini DJ, Shah NG, Wach A, Brachat A, Philippsen P, Pringle JR (1998). Additional modules for versatile and economical PCR-based gene deletion and modification in *Saccharomyces cerevisiae*. Yeast 14, 953–961.
Maiato H, Gomes AM, Sousa F, Barisic M (2017). Mechanisms of chromosome congression during mitosis. In Biology 6. https://doi.org/10.3390/biology6010013
Marco E, Dorn JF, Hsu PH, Jaqaman K, Sorger PK, Danuser G (2013). *S. cerevisiae* chromosomes biorient via gradual resolution of syntely between S phase and anaphase. Cell 154. https://doi.org/10.1016/j.cell.2013.08.008
Markus SM, Omer S, Baranowski K, Lee WL (2015). Improved plasmids for fluorescent protein tagging of microtubules in *Saccharomyces cerevisiae*. Traffic 16, 773–786.
Miller RK, D'Silva S, Moore JK, Goodson HV. (2006). The CLIP-170 orthologue Bik1p and positioning the mitotic spindle in yeast. In Curr Top Dev Biol 76. https://doi.org/10.1016/S0070-2153(06)76002-1
Molk JN, Salmon ED, Bloom K (2006). Nuclear congression is driven by cytoplasmic microtubule plus end interactions in *S. cerevisiae*. J Cell Biol 172. https://doi.org/10.1083/jcb.200510032
Moore JK, D'Silva S, Miller RK (2006). The CLIP-170 homologue Bik1p promotes the phosphorylation and asymmetric localization of Kar9p. Mol Biol Cell 17. https://doi.org/10.1091/mbc.E05-06-0565
O'Toole ET, Winey M, McIntosh JR (1999). High-voltage electron tomography of spindle pole bodies and early mitotic spindles in the yeast Saccharomyces cerevisiae. Mol Biol Cell 10. https://doi.org/10.1091/mbc.10.6.2017
Pandey H, Reithmann E, Goldstein-Levitin A, Al-Bassam J, Frey E, Gheber L (2021). Drag-induced directionality switching of kinesin-5 Cin8 revealed by cluster-motility analysis. Sci Adv 7. https://doi.org/10.1126/sciadv.abc1687
Pearson CG, Gardner MK, Paliulis LV, Salmon ED, Odde DJ, Bloom K (2006). Measuring nanometer scale gradients in spindle microtubule dynamics using model convolution microscopy. Mol Biol Cell 17. https://doi.org/10.1091/mbc.E06-04-0312
Peterson JB, Ris H (1976). Electron microscopic study of the spindle and chromosome movement in the yeast *Saccharomyces cerevisiae*. J Cell Sci 22.
Powers AF, Franck AD, Gestaut DR, Cooper J, Gracyzk B, Wei RR, Wordeman L, Davis TN, Asbury CL (2009). The Ndc80 kinetochore complex forms load-bearing attachments to dynamic microtubule tips via biased diffusion. Cell 136. https://doi.org/10.1016/j.cell.2008.12.045
Roberts AJ, Goodman BS, Reck-Peterson SL (2014). Reconstitution of dynein transport to the microtubule plus end by kinesin. ELife 3. https://doi.org/10.7554/elife.02641
Roostalu J, Hentrich C, Bieling P, Telley IA, Schiebel E, Surrey T (2011). Directional switching of the kinesin Cin8 through motor coupling. Science 332. https://doi.org/10.1126/science.1199945
Roux KJ, Kim DI, Raida M, Burke B (2012). A promiscuous biotin ligase fusion protein identifies proximal and interacting proteins in mammalian cells. J Cell Biol 196. https://doi.org/10.1083/jcb.201112098
Schindelin J, Arganda-Carreras I, Frise E, Kaynig V, Longair M, Pietzsch T, Preibisch S, Rueden C, Saalfeld S, Schmid B, *et al*. (2012). Fiji: an open-source platform for biological-image analysis. In Nature Methods 9. https://doi.org/10.1038/nmeth.2019
Shyu YJ, Hu CD (2008). Fluorescence complementation: an emerging tool for biological research. In Trends Biotechnol 26. https://doi.org/10.1016/j.tibtech.2008.07.006
Sprague BL, Pearson CG, Maddox PS, Bloom KS, Salmon ED, Odde DJ (2003). Mechanisms of microtubule-based kinetochore positioning in the yeast metaphase spindle. Biophys J 84. https://doi.org/10.1016/S0006-3495(03)75087-5
Su X, Qiu W, Gupta ML, Pereira-Leal JB, Reck-Peterson SL, Pellman D (2011). Mechanisms underlying the dual-mode regulation of microtubule dynamics by Kip3/Kinesin-8. Mol Cell 43. https://doi.org/10.1016/j.molcel.2011.06.027
Sung MK, Huh WK (2007). Biomolecular fluorescence complementation analysis system for in vivo detection of protein–protein interaction in *Saccharomyces cerevisiae*. Yeast 24. https://doi.org/10.1002/yea.1504
Suzuki A, Badger BL, Haase J, Ohashi T, Erickson HP, Salmon ED, Bloom K (2016). How the kinetochore couples microtubule force and centromere stretch to move chromosomes. Nat Cell Biol 18. https://doi.org/10.1038/ncb3323
Suzuki A, Gupta A, Long SK, Evans R, Badger BL, Salmon ED, Biggins S, Bloom K (2018). A Kinesin-5, Cin8, recruits protein phosphatase 1 to kinetochores and regulates chromosome segregation. Curr Biol 28. https://doi.org/10.1016/j.cub.2018.08.038
Tanaka TU, Stark MJR, Tanaka K (2005). Kinetochore capture and bi-orientation on the mitotic spindle. Nat Rev Mol Cell Biol 6, 929–942.
Tong AHY, Lesage G, Bader GD, Ding H, Xu H, Xin X, Young J, Berriz GF, Brost RL, Chang M, *et al*. (2004). Global mapping of the yeast genetic interaction network. Science 303. https://doi.org/10.1126/science.1091317
Tytell JD, Sorger PK (2006). Analysis of kinesin motor function at budding yeast kinetochores. J Cell Biol 172. https://doi.org/10.1083/jcb.200509101
Varga V, Helenius J, Tanaka K, Hyman AA, Tanaka TU, Howard J (2006). Yeast kinesin-8 depolymerizes microtubules in a length-dependent manner. Nat Cell Biol 8. https://doi.org/10.1038/ncb1462
Wargacki MM, Tay JC, Muller EG, Asbury CL, Davis TN (2010). Kip3, the yeast kinesin-8, is required for clustering of kinetochores at metaphase. Cell Cycle 9. https://doi.org/10.4161/cc.9.13.12076
Winey M, Mamay CL, O'Toole ET, Mastronarde DN, Giddings TH, McDonald KL, McIntosh JR (1995). Three-dimensional ultrastructural analysis of the *Saccharomyces cerevisiae* mitotic spindle. J Cell Biol 129. https://doi.org/10.1083/jcb.129.6.1601
Winey M, O'Toole ET (2001). The spindle cycle in budding yeast. In Nat Cell Biol 3. https://doi.org/10.1038/35050663
Xiang X (2018). Nuclear movement in fungi. In Semin Cell Dev Biol 82. https://doi.org/10.1016/j.semcdb.2017.10.024